LESSONS LEARNED FROM RANS SIMULATIONS OF SHOCK-WAVE/BOUNDARY-LAYER INTERACTIONS

Frédéric Thivet*
ONERA, Centre de Toulouse, 31055 Toulouse, France

Usual two-equation turbulence models, based on a constant value of c_μ in the definition of the eddy viscosity, are known to fail in predicting most features of Shock-Wave/Boundary-Layer Interactions (SWBLI). In searching a simple way to improve their capabilities, it appears that three different theoretical approaches end up with simple and similar Weakly Non-Linear (WNL) corrections. Such a correction, originally proposed to ensure realizability in subsonic flows, is extended to deal with compressible flows and applied to three-dimensional supersonic SWBLI developing on three single sharp fin plate configurations. The numerical solutions are obtained by solving the full Reynolds-Averaged Navier-Stokes equations on grids up to 3.3 million cells with the linear and WNL versions of the $k-\omega$ turbulence model. The WNL correction allows full grid-convergence and yields much better numerical solutions, including the prediction of the pressure plateau under the lambda foot of the shock, the maximum skin-friction coefficient on the bottom plate, and the secondary separation in the strong SWBLI case. The improvement is due to halving the turbulence intensity in the vortical flow embedded within the lambda foot of the shock. The WNL correction has also a beneficial effect in transonic cases, as illustrated for a two-dimensional channel flow over a bump. Finally, its success in predicting unsteady features in the case of shock-induced oscillations in transonic flows over airfoils is underlined. In the considered 3-D supersonic, 2-D transonic steady and unsteady SWBLI, the key-point is the dependency of c_μ on the strain and vorticity invariants rather than the non-linear expansion of the shear stress.

Introduction

One of the main issues faced by turbulence modeling is to predict the behavior of flows in presence of large pressure gradients, in particular when yielding a boundary-layer separation. Because they appear in many aeronautical applications, and because they include very large pressure gradients, Shock-Wave/Boundary-Layer Interactions (SWBLI) are a very interesting archetype of such flows. In a comprehensive and recent review, Dolling[1] underlines the main features of these flows that cannot be predicted today: heat transfer, skin friction and unsteady pressure loads. The most recent monographs on the subject are due to Délery & Panaras[2] and Smits & Dussauge.[3] The last review of computational capabilities for SWBLI is due to Knight & Degrez,[4] and the next one will come from the RTO/AVT Working Group 10. Specifically for sharp fin plate interactions, recent and thorough analyses can be found in Refs. 5–7 for single fins, and Refs. 8–13 for double fins.

Usual turbulence models, among which most of two-equation turbulence models, are based on the linear formulation of the Boussinesq assumption: the Reynolds stress is directly proportional to the mean strain rate. In the following, such models are called linear, while models not observing the linear Boussinesq assumption are called non-linear. Linear models usually fail in predicting the boundary-layer separation or the level of the turbulent kinetic energy (and consequently skin friction and heat transfer) in SWBLI. To overcome the difficulties encountered by Reynolds-averaged Navier-Stokes (RANS) solvers, Knight & Degrez[4] recommend developing Large-Eddy Simulation solvers. This is currently carried out, with applications to two-dimensional compressible high-speed flows.[14–16] However, the way still seems to be long before these techniques become reliable and affordable in complex three-dimensional configurations. On the RANS side, a lot of efforts is put in deriving non-linear turbulence models, either in an explicit algebraic form or through transport equations for the Reynolds stress components. These models contain many empirical constants and damping functions near walls, which are not easy to determine individually from a set of experiments. This on-going research has not yet reached a point where a unique formulation could be able to model a very large range of flow configurations. In consequence, Non-Linear Eddy-Viscosity Models or Reynolds-Stress Transport-Equation Models still belong to the research community and are not yet used intensively for engineering applications. The aim of this paper is to point out some intermediate model, between usual linear two-equation models and fully non-linear models, which would yield better predictions of SWBLI than linear models, and would be much simpler and more reliable than current non-linear models. The idea is to identify a correction to linear models which could be viewed as the first-order term of their difference to non-linear models. Such a correction has been recently pointed out after a parametric study of realizability corrections.[17] It is proven to be useful to improve the prediction of

*Senior Research Engineer, Department of Aerodynamics and Energetics Modeling. AIAA Member.

Report Documentation Page

Form Approved
OMB No. 0704-0188

1. REPORT DATE	2. REPORT TYPE	3. DATES COVERED
01 JAN 2006	**N/A**	**-**

4. TITLE AND SUBTITLE	5a. CONTRACT NUMBER
Lessons Learned from RANS Simulations of Shock-Wave/Boundary-Layer Interactions	5b. GRANT NUMBER
	5c. PROGRAM ELEMENT NUMBER
6. AUTHOR(S)	5d. PROJECT NUMBER
	5e. TASK NUMBER
	5f. WORK UNIT NUMBER
7. PERFORMING ORGANIZATION NAME(S) AND ADDRESS(ES) **ONERA, Centre de Toulouse, 31055 Toulouse, France**	8. PERFORMING ORGANIZATION REPORT NUMBER
9. SPONSORING/MONITORING AGENCY NAME(S) AND ADDRESS(ES)	10. SPONSOR/MONITOR'S ACRONYM(S)
	11. SPONSOR/MONITOR'S REPORT NUMBER(S)

12. DISTRIBUTION/AVAILABILITY STATEMENT
Approved for public release, distribution unlimited

13. SUPPLEMENTARY NOTES
See also ADM001860, Technologies for Propelled Hypersonic Flight (Technologies des vols hypersoniques propulses). , The original document contains color images.

14. ABSTRACT

15. SUBJECT TERMS

16. SECURITY CLASSIFICATION OF:			17. LIMITATION OF ABSTRACT	18. NUMBER OF PAGES	19a. NAME OF RESPONSIBLE PERSON
a. REPORT	b. ABSTRACT	c. THIS PAGE			
unclassified	**unclassified**	**unclassified**	**UU**	**12**	

wall heat fluxes in Crossing SWBLI. Moreover, it is shown that no other usual compressibility correction or turbulent lenght-scale limit can further improve the results. Here, different ways of building Weakly Non-Linear (WNL) corrections are examined, together with the applications they have been designed for, in order to underline the currently known applicability of the proposed correction. Then a new set of computations about single sharp fin plate SWBLI is analyzed to assess the ability of the WNL correction to solve the SWBLI skin-friction issue. Finally, the effect of the correction is presented for steady and unsteady transonic interactions.

Ways Toward Weakly Non-Linear Turbulence Models

Linear Models and the Bradshaw's Assumption

Usual turbulence models are based on a linear relationship between the turbulent stresses and the mean strain rate derived from the Boussinesq's assumption. If u_i is the fluctuation of the mass-averaged velocity field U_i, the deviation of the turbulent stress writes:

$$-\rho\widetilde{u_i u_j} + \frac{2}{3}\rho k\,\delta_{ij} = 2\,\mu_t\left(S_{ij} - \frac{1}{3}S_{kk}\,\delta_{ij}\right) \qquad (1)$$

where the mean strain is:

$$S_{ij} = \frac{1}{2}\left(\frac{\partial U_i}{\partial x_j} + \frac{\partial U_j}{\partial x_i}\right) \qquad (2)$$

The eddy viscosity μ_t depends only on turbulent scales, such as the turbulent kinetic energy k (TKE) and its specific dissipation ω:

$$\mu_t = \rho\,c_\mu\,\frac{k}{\omega} \qquad (3)$$

Usually, c_μ is set to the constant value $c_\mu^\circ = 0.09$ which is adequate to model the flat plate boundary layer. However, this assumption is known to be highly unrealistic in presence of adverse pressure gradients. In a two-dimensional boundary layer, the shear stress is no more proportional to the velocity gradient but to the TKE:

$$-\widetilde{uv} = \sqrt{c_\mu^\circ}\;k \qquad (4)$$

as pointed out by Bradshaw.[18] The simplest frame-independent way to reconcile both expressions is to introduce a weak non-linearity in the eddy viscosity, such as:

$$c_\mu = \min\left\{c_\mu^\circ,\ \frac{\sqrt{c_\mu^\circ}}{s}\right\} \qquad (5)$$

which involves the dimensionless mean strain rate:

$$s = \frac{S}{\omega} \quad \text{with} \quad S^2 = 2S_{ij}S_{ji} - \frac{2}{3}S_{kk}^2 \qquad (6)$$

This idea, originally proposed by Coakley for incompressible flows,[19] was used again by Menter[20] to define the $k-\omega$ Shear-Stress Transport (SST) model. The only difference in c_μ is that, in extending the velocity gradient $\partial U/\partial y$ to three dimensions, Menter chose the vorticity invariant:

$$\varpi = \frac{\sqrt{2\Omega_{ij}\Omega_{ji}}}{\omega} \quad \text{where} \quad \Omega_{ij} = \frac{1}{2}\left(\frac{\partial U_i}{\partial x_j} - \frac{\partial U_j}{\partial x_i}\right) \qquad (7)$$

in Eq. (5) instead of the strain rate invariant s.

Link with Realizability

A well-known example of problems encountered in flows with strong velocity gradients (and streamline curvature) is the stagnation-point anomaly: near the stagnation point of an impinging jet[21] or a turbine blade,[22] linear two-equation models overstimate the TKE level by orders of magnitude. In the case of an impinging jet, the heat-transfer coefficient is systematically overestimated. Based on the realizability principle,[23] a minimal correction was derived for two-equation turbulence models and was shown to cure the stagnation-point anomaly[21] and to solve the jet-impingement problem.[24] Although starting from the theoretical realizability principle rather than the empirical Bradshaw's assumption, Durbin ends up with a correction which is formally identical to Coakley's proposal:

$$c_\mu = \min\left\{c_\mu^\circ,\ \frac{c}{s\sqrt{3}}\right\} \quad \text{with} \quad c = \frac{1}{2} \qquad (8)$$

for which the constant $c/\sqrt{3} = 0.29$ is very close to $\sqrt{c_\mu^\circ} = 0.30$.* More elaborate expressions of c_μ have been derived to respect the realizability principle, including formula where $\sqrt{(s^2+\varpi^2)/2}$ is substituted to s in Eq. (8) in order to account for some three-dimensional and rotational effects.[22] In most cases, including those considered here, both expressions are equivalent. Whatever the expression, the essential point is to reproduce the asymptotic behavior of c_μ when s or $\sqrt{(s^2+\varpi^2)/2}$ tends toward infinity.

The model is completed with the transport equations:

$$D_t(\rho k) = P_k - \beta^\star\rho k\omega + \frac{\partial}{\partial x_j}\left[(\mu + \sigma^\star\mu_t)\,\frac{\partial k}{\partial x_j}\right] \qquad (9)$$

$$D_t(\rho\omega) = \underbrace{\alpha\frac{\omega}{k}\left(\frac{P_{ki}}{\boldsymbol{\alpha_\nu}} + P_{kc}\right)}_{P_\omega} - \underbrace{\beta\rho\omega^2}_{D_\omega} + \frac{\partial}{\partial x_j}\left[(\mu+\sigma\mu_t)\,\frac{\partial\omega}{\partial x_j}\right] \qquad (10)$$

where the constants from the original model are: $\alpha = 5/9$, $\beta = 5/6$, $\beta^\star = 1$, $\sigma = \sigma^\star = 1/2$, and the TKE production rate is:

$$P_k = \underbrace{\mu_t S^2}_{P_{ki}} \underbrace{- \frac{2}{3}\rho k\,S_{kk}}_{P_{kc}} \qquad (11)$$

*In Eq. (8), only $c \le 1$ is needed to ensure realizability; the value $c = 1/2$ is required to obtain a better fit of heat-transfer coefficient measurements in impinging jets.[24]

Different ways may be found to write the net production rate of the dissipation. Coakley[19] and Moore & Moore[22] do not modify the formal expression of the transport equation for the dissipation ($\alpha_\nu = 1$ in Eq. (10)). Consequently, the decrease in μ_t propagates to both TKE and dissipation production rates through Eq. (11). Menter in the SST model[20] and Durbin[21] divide the production rate of the dissipation by $\alpha_\nu = c_\mu / c_\mu^\circ$, so that the resulting production rate P_ω is basically unaffected by the WNL correction. This way, the effect of the correction is strengthened because the production of TKE is lowered and the production of dissipation is not. This choice is adopted here, but for the compressible part of P_ω, *i.e.* $\alpha(\omega/k)P_{kc}$, which is not divided by α_ν because it does not depend directly on μ_t. Durbin[21] also recommends dividing the dissipation rate of the dissipation D_ω by α_ν. This is not justified by any dependency of D_ω on μ_t, so that this choice is not retained here, which further strengthens the effect of the WNL correction.

Link with Non-Linear Models

The link of the Weakly Non-Linear correction (8) with fully non-linear models is clearly pointed out in the work by Pope,[28] when deriving an effective viscosity more general than the linear Boussinesq assumption: the first term in the full development of the Reynolds stress has the same form as proposed here.

Successfull Applications of WNL Corrections

The preceeding analysis shows that 1) the generalization of the empirical Bradshaw's assumption, 2) the enforcement of the realizability principle, and 3) the search for the most general effective eddy viscosity all end up with very similar dependencies of c_μ on the strain rate and vorticity invariants in two-equation turbulence models. These expressions have been successfully used to improve the prediction of flows with strong velocity gradients such as flows over turbine blades,[22] airfoils in a turbulent freestream[21] and impinging jets.[24] In Crossing SWBLI, the proposed WNL correction has been shown to efficiently suppress the violation of realizability and to improve the prediction of wall pressure and heat-transfer coefficient, even though further progress is still needed.[17] In the next section, the ability of the correction to address the pressure and skin-friction issues in 3-D SWBLI is assessed.

Performance of WNL Models in Single Fin SWBLI

Single Sharp Fin Plate Experiments

The single fin plate interaction is representative of flows developing over many elements of supersonic bodies, such as inlets, fuselage/wing junctions, control surfaces... In this configuration using a simple geometrical definition (Fig. 1), the shock sheet emanating from the fin leading edge interacts with the incoming boundary layer developing along the bottom wall. The boundary layer separates and the foot of the shock takes a lambda shape. Experiments, and then computations, have revealed the vortical nature of the flow embedded within the lambda foot. The classification of the secondary separation development stages has been established by Zheltovodov:[25] types I and II correspond to weak interactions without secondary separation; when the interaction strength increases, a secondary separation first appears below the vortical flow (type III), then tends to disappear (types IV, V) and re-appears closer to the fin for very strong interactions (type VI). The attachment of the vortical flow on the bottom plate yields large peaks in pressure and skin-friction coefficient. The primary features of the interactions (wall pressure distribution, primary separation and attachment lines) are fairly well predicted by RANS computations.[4] However, the skin-friction peak is overestimated, often by more than 50 %, and no model has been yet shown to be able to predict the secondary separation appearance/disappearance/re-appearance phenomenon.[5] Here, three configurations denoted SF315, SF420 and SF430 (Table 1), are selected to reproduce the interactions of type III, IV and VI.

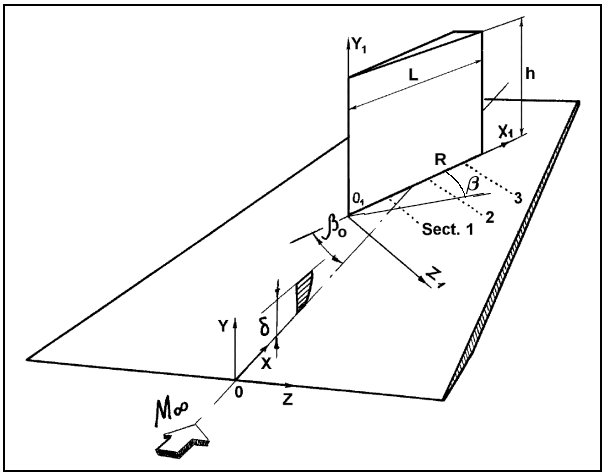

Fig. 1 Single sharp fin plate configuration.

Numerical Method

The three-dimensional compressible steady RANS equations are solved using the code GASPex.[29] The inviscid fluxes are computed to third-order accuracy using the Roe scheme and a MUSCL reconstruction method with the Min-Mod limiter. Turbulence is represented using the Wilcox' $k-\omega$ model,[30] implemented with the smooth wall boundary condition[31] and denoted WI. The weakly non-linear version of this model, denoted WD$^+$,[17] is the extension to compressible flows of the non-linear correction of Durbin[21] as described above. The subsequent results are affected neither by the wall condition nor the freestream condition on the $k-\omega$ model, in the limits given in Ref. 32.

Table 1 Single sharp fin plate flow features: Mach number, fin angle, total temperature, stagnation pressure, station of the boundary layer measurements, Mach number at this station, wall temperature, unit Reynolds number, boundary layer thickness, momentum thickness.

Case	M_∞	$\beta_\circ$ (deg.)	$T_{i\infty}$ (K)	$P_{i\infty}$ (kPa)	$X_\circ$ (mm)	$M_\circ$	T_w (K)	$R_{u\circ}$ (10^6/m)	$\delta_\circ$ (mm)	$\theta_\circ$ (mm)
SF315 (Ref. 25)	3	15	283	422	-4	2.87	265	36.56	5.3	0.36
SF420 (Ref. 26)	3.97	20	293	1524	38	3.97	283	72.25	2.87	0.128
SF430 (Ref. 27)	4	30.6	283	610	0	3.77	260	33.63	4.9	0.29

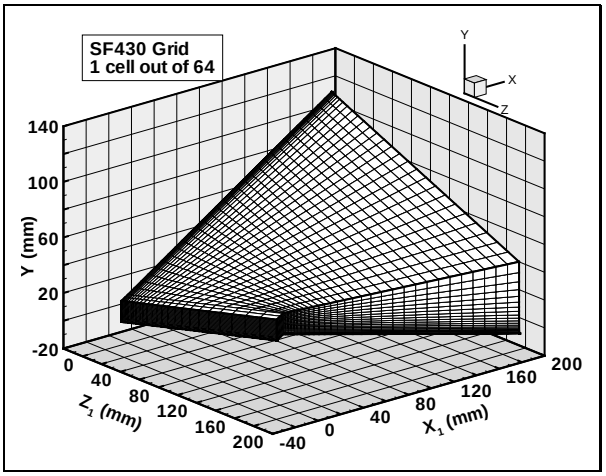

Fig. 2 Single sharp fin plate, example of grid.

The inflow and lateral conditions correspond to a previously computed flat plate boundary layer matching the momentum thickness as measured in the experiments. The computational domain is limited to the region influenced by the interaction (Fig. 2). The longitudinal step is about one third of the Incoming Boundary Layer (IBL) thickness. In the direction normal to the bottom plate, 100 cells out of 160 are exponentially distributed along the IBL height. The first cell height is 0.18 μm in the SF315 case (resp. 0.10 μm and 0.15 μm in the SF420 and SF430 cases). It represents less than 0.05 wall units in the IBL. The maximum height in wall units on the bottom plate is 0.24 and it is reached along the attachment line. In the transverse direction, one half of the 160 cells is concentrated within the side-wall boundary layer with a first cell width of about the double of the first cell height. The total number of cells is around 3.3 million ($128 \times 160 \times 160$) in the SF315 and SF430 cases, 2.8 million ($112 \times 160 \times 160$) in the SF420 case.

Solving the Grid-Convergence Issue

The mesh-sequencing technique[29] is used to assess the grid-convergence of the solutions. The preceeding description corresponds to the very fine level of the grids ($N_x \times 160 \times 160$). The fine level ($N_x \times 80 \times 80$) is obtained by merging the cells two by two in both normal and transverse directions. Medium ($N_x \times 40 \times 40$) and coarse levels ($N_x \times 20 \times 20$) are defined by repeating the same procedure. Steady solutions are obtained on all four levels, from the coarser to the finer. Figure 3

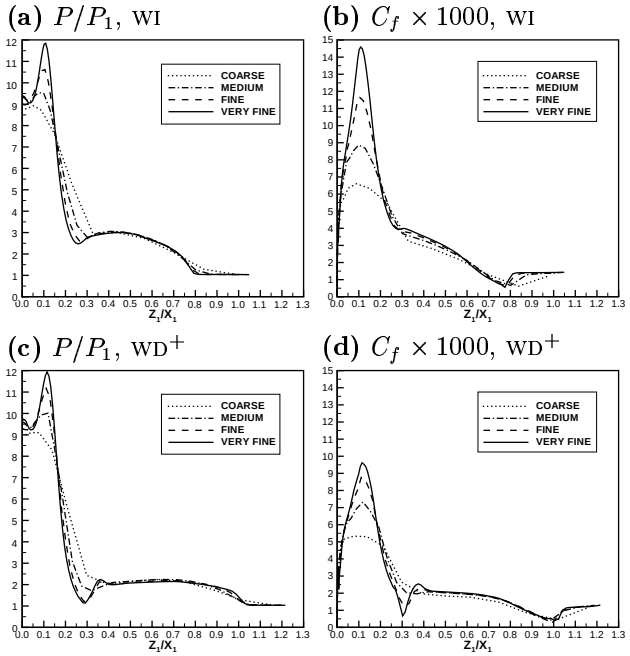

Fig. 3 Grid convergence for the SF430 configuration at the wall in the cross-section $X_1 = 122.5$ mm.

shows the wall distribution of pressure (normalized by the pressure in the IBL) and skin-friction coefficient in cross-section $X_1 = 122.5$ mm of the SF430 configuration. It demonstrates that with the WI model, grid-convergence is achieved very fast everywhere, except in the vicinity of the attachment line $Z_1/X_1 \simeq 0.1$. In this region, a constant growth in skin-friction coefficient (Fig. 3b) and even pressure (Fig. 3a) is observed when grid is refined. This misbehavior is cured by the WNL correction as illustrated by Figs. 3c and 3d showing that the solution on the very-fine grid is grid-converged everywhere.

This has to be related to the fact that some terms in the turbulent equations of a linear two-equation model tend toward infinity across the shock when grid is refined. For instance, if $\Delta\xi$ is the width of the cell crossed by the shock wave, and if Δv is the corresponding finite jump in velocity, the gradients verify:

$$S^2 \sim \frac{4}{3}\left(\frac{\Delta v}{\Delta \xi}\right)^2 \quad \text{and} \quad S_{kk} \sim \frac{\Delta v}{\Delta \xi} \qquad (12)$$

Consequently, the asymptotic behavior of the incompressible and compressible parts of the TKE produc-

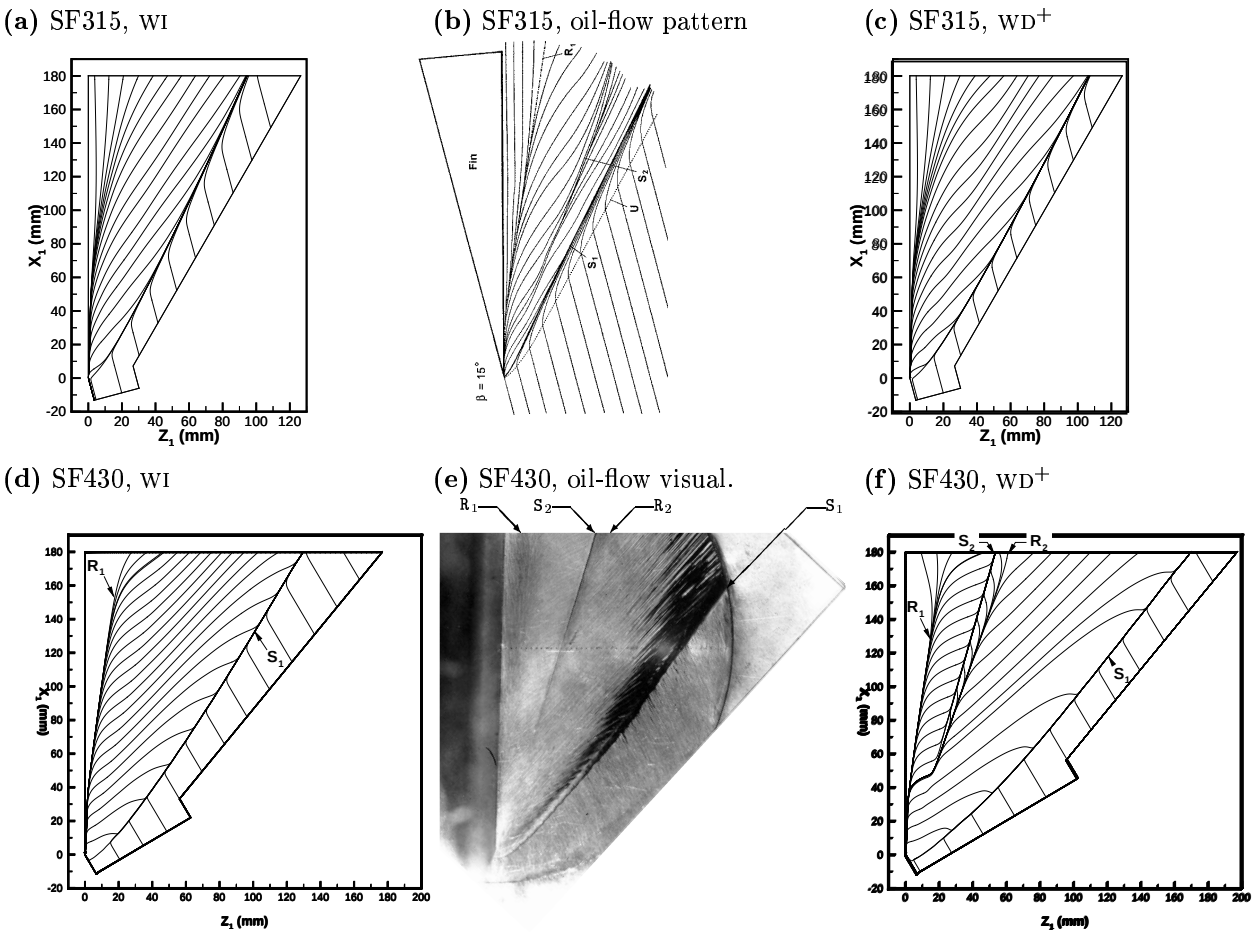

Fig. 4 Skin-friction lines on the bottom plate of single sharp fin plate configurations (Top views).

tion rate, integrated over the cell volume is:

$$\int P_{ki}\, dV \sim \frac{4}{3}\,\rho k\,\frac{c_\mu}{\omega}\,\frac{\Delta v}{\Delta \xi}\,\Delta v \qquad (13)$$

$$\int P_{kc}\, dV \sim -\frac{2}{3}\,\rho k\,\Delta v \qquad (14)$$

With a linear Boussinesq model ($c_\mu = c_\mu^\circ$), $\int P_k\, dV$ behaves as $1/\Delta\xi$ in the cell crossed by the shock wave. This unphysical behavior prevents grid-convergence. With the WNL correction Eq. (8), $\int P_k\, dV$ tends toward the finite value $(2/3)\,(c-1)\,\rho k\,\Delta v$ when grid is refined ($\Delta\xi$ tends toward 0). Then, grid-convergence becomes possible. In most configurations, the misbehavior of the TKE production rate has no practical consequence, because the fluid crossing the shock wave does not reach the regions under observation. However, in the considered SWBLI, the fluid originating from the upper part of the boundary layer crosses the lambda-foot shock and is entrained by the primary vortex toward the bottom wall that it impinges along the attachment line.[17] It becomes highly probable that a flaw in grid-convergence near the shock is reflected in the solution along the attachment line.

Solving the Secondary Separation Issue

Views of the skin-friction lines on the bottom plate are reported in Fig. 4 in the weak (SF315) and strong (SF430) interaction cases. The angles of the attachment and separation lines with respect to the incoming flow direction are reported in Table 2. The domain under influence of the interaction is bounded by the primary separation line S_1. Its angle is systematically underestimated by the linear model by 1.5° to 4° and overestimated by the WD$^+$ model by 1° to 2.5°. The angle of the primary attachment line R_1 is correctly

Configuration		PA	SS	SA	PS
SF315	EXP	23.5	36.5	—	41.5
	WI	24.0	—	—	40.0
	WD$^+$	23.0	27–31	—	42.5
SF420	EXP	25.0	39.0	—	46.0
	WI	26.0	—	—	44.5
	WD$^+$	26.0	—	—	47.5
SF430	EXP	37.0	46.5	48.0	66.0
	WI	38.8	—	—	62.0
	WD$^+$	39.5	47.0	50.5	68.5

Table 2 Angles of Primary Attachment (PA), Secondary Separation (SS), Secondary Attachment (SA), and Primary Separation (PS) lines.

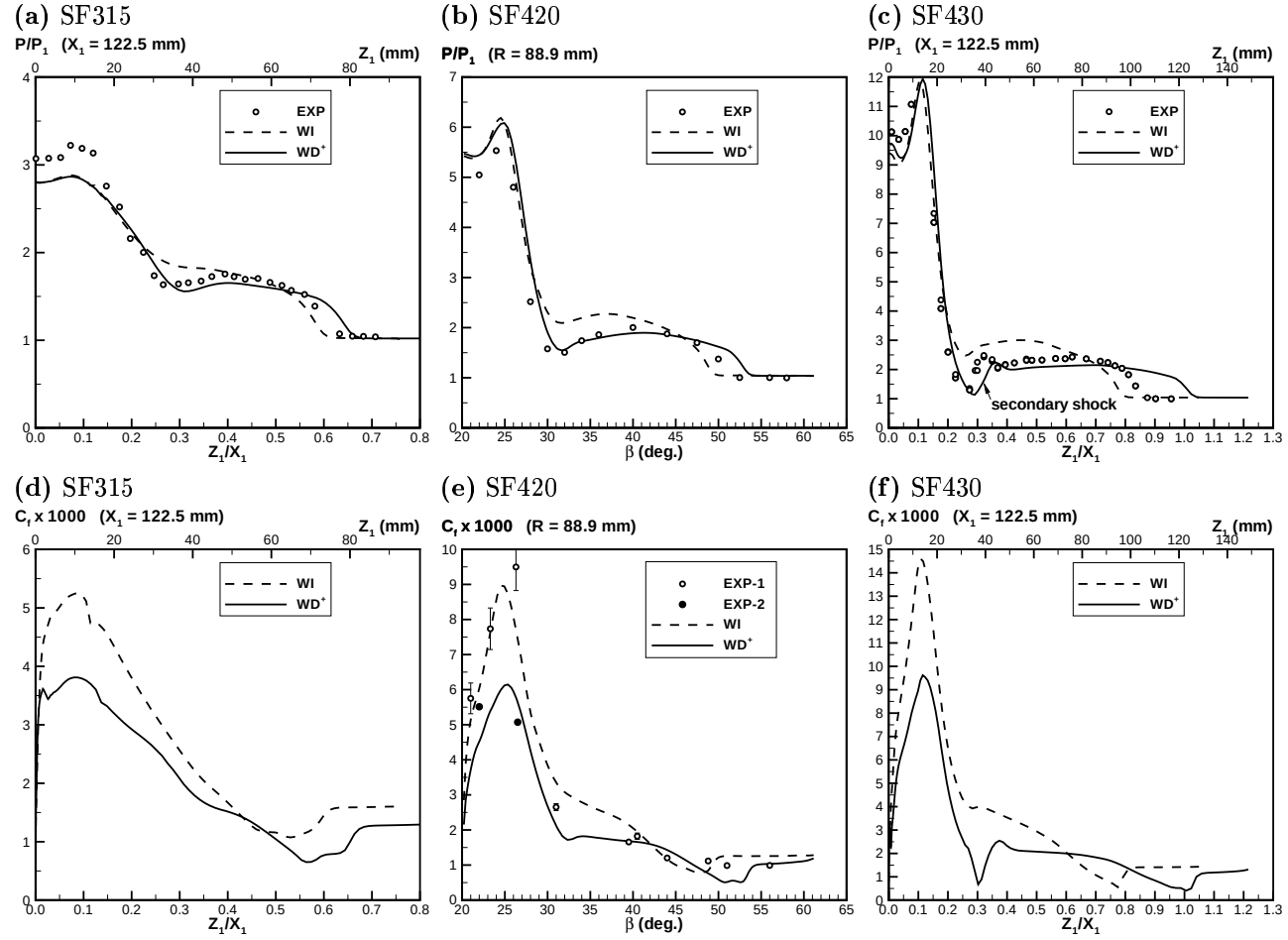

Fig. 5 Wall pressure and skin-friction coefficient in cross-sections of single sharp fin plate configurations.

predicted by both models. In the type VI interaction (SF430), the secondary separation and re-attachment lines S_2 and R_2 visible in the experiment (Fig. 4e) are obviously predicted by the WD$^+$ model (Fig. 4f) while they are missed by the WI model (Fig. 4d). The angles of these lines are very close to the measurements (Table 2). Now, in the type III interaction (SF315), the other kind of secondary separation as observed in the experiment (Fig. 4b) is absent from both numerical solutions. Nevertheless, the WD$^+$ model gives an obvious deviation of the skin-friction lines (Fig. 4c), which indicates a good tendency of the model.

Solving the Pressure and Skin-Friction Issues

The WNL correction has also a beneficial effect on the pressure distribution. In Figs. 5a–5c, the computed pressures on the bottom plate are compared with measurements along cross-sections normal to the fin surface. The cross-section line is straight in the SF315 and SF430 cases (Figs. 5a, 5c) and circular in the SF420 case (Fig. 5b). The geometrical variables X_1, Z_1, R and β are defined in Fig. 1. The prediction of the pressure plateau under the vortical flow embedded within the lambda foot of the shock is poor without the WNL correction and very good with it (SF315: $Z_1/X_1 = 0.35 - 0.55$, SF420: $\beta = 35 - 50°$, SF430: $Z_1/X_1 = 0.35 - 0.8$). Figures 5a–5c confirm that the interaction extent (the region where the pressure differs from its level in the IBL) is overestimated with the WNL model and underestimated without it.

The local dip in pressure observed between the attachment and the vortical flow is well predicted by the WD$^+$ model while it is missed by the linear model (SF315, SF430: $Z_1/X_1 \simeq 0.3$, SF420: $\beta \simeq 32°$). In the strong interaction case, the WD$^+$ model gives the secondary shock and the weak local peak in pressure associated with the secondary re-attachment (Fig. 5c, $Z_1/X_1 \simeq 0.35$).

Finally, the pressure distribution between the fin and the primary attachment line is nearly the same in both numerical solutions. The peak value of the pressure is underestimated by about 9% in the mild interaction (SF315), and overestimated by about 5% in the strong interactions (SF420 and SF430).

Figures 5d–5f show the skin-friction coefficient C_f in the same cross-sections as for the wall pressure. The major effect of the WNL correction is to decrease the maximum in C_f by 30 to 35 %. In the SF420 case, two series of measurements are reported (Fig. 5e). The second one (closed circles labelled EXP-2) resulted in

corrected values of the skin-friction coefficient near the primary attachment line.[4] The WD$^+$ solution agrees well with the correct measurements. The WI model, like other linear two-equation models[4] or even the Baldwin and Lomax model as modified by Panaras,[6] yields an overestimate by at least 50% of the maximum skin-friction coefficient. Some other models of $k-\epsilon$ type do not exhibit this erroneous peak value, but the overall C_f distribution is quite far from the measurements (Ref. 4, Fig. 50). Although measurements are not available in the SF430 case, the reduction in C_f near $Z_1/X_1 \simeq 0.35$ (Fig. 5f) is validated by the subsequent appearance of the secondary separation and re-attachment lines (Fig. 4e, 4f).

Reducing the Turbulent Kinetic Energy Level

Figure 6a shows the WNL correction factor $\alpha_\nu = c_\mu/c_\mu^\circ$ in cross-section $X_1 = 122.5$ mm of the SF430 configuration. The WNL correction is active (*i.e.* α_ν is smaller than 1) only through the legs of the shock wave and also in the core of the vortical flow and near the attachment line. The effect on the turbulence intensity k/U_∞^2 is dramatic : the maximum, achieved in the core of the vortex, is more than halved by the WNL correction (Figs. 6b, 6c). Consequently, the intensity of the rear-leg shock is larger, the secondary shock can appear and the primary vortex is flatter. The action of the WNL correction through the foreleg of the shock yields the observed wider extent of the interaction. Due to the sensitivity of the solution in this region, only a very slight change in the correction should be sufficient to improve the prediction of the interaction extent.

(a) WD$^+$, WNL factor $\alpha_\nu = c_\mu/c_\mu^\circ$

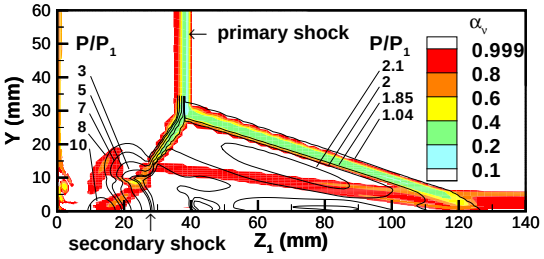

(b) WI, turbulence intensity k/U_∞^2

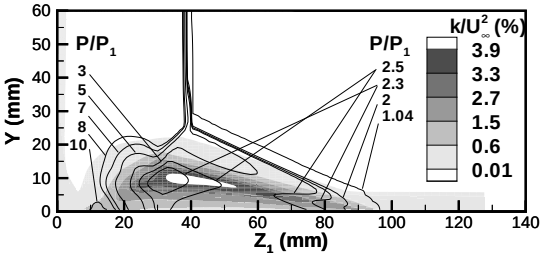

(c) WD$^+$, turbulence intensity k/U_∞^2

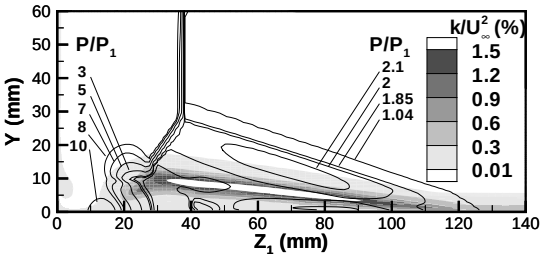

Fig. 6 Turbulent quantities in cross-section $X_1 = 122.5$ mm of SF430 configuration.

Performance of WNL Models in Transonic Flows

The identified WNL correction has been successfully used in supersonic SWBLI. It was initially designed to handle subsonic configurations with highly curved streamlines around stagnation points. In order to complete the validation, transonic cases have to be considered as well. The purpose of this section is to assess the behavior of the WNL correction in two different transonic SWBLI. The second configuration is chosen to give a flavor of the interest of weakly nonlinear models for unsteady flows.

Transonic SWBLI in a Channel Flow

The first transonic configuration is a two-dimensional channel flow with a bump on the lower wall (Fig. 7). The channel inlet Mach number is 0.615 with a total pressure of 96 kPa and a total temperature of 300 K; the back pressure is set to 61.5 kPa. The experimental study due to Délery[33] shows that along the bump ramp, the flow accelerates and reaches a Mach number of about 1.4. A shock forms to accomodate the back pressure. On the lower wall, above the downstream part of the bump, the shock-wave/boundary-layer interaction causes the separation of the boundary layer, the formation of a recirculation bubble and a large lambda-foot shock (Fig. 8a). This configuration has been considered in several computational workshops,[35,36] from which it results that no linear two-equation model nor tested Reynolds-Stress model is able to reproduce the correct large lambda shock visible in the experiment nor the pressure plateau underneath. Only the SST $k-\omega$ model and the cubic Non-Linear Eddy-Viscosity Model (NLEVM) by Craft *et al.*[37] show some ability to exhibit these features.[36]

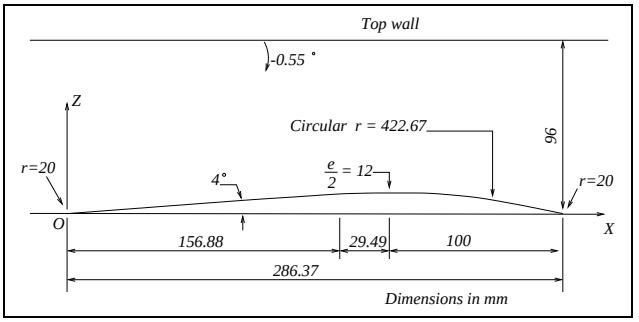

Fig. 7 Geometry of the transonic bump[33] (from Ref. 34, with permission).

In a recent numerical study discussed hereafter, Dieudonné[34] contributes to a better understanding of the situation. Across both legs of the lambda shock, the TKE production term given by the usual linear stress-strain relation grows unbounded. Consequently, the eddy viscosity is too high and prevents the development of the lambda shape of the shock. Figure 8b shows a typical result from linear two-equation models. This one is obtained with the WI $k-\omega$ model. By adding the SST correction, a much better lambda shape is obtained (Fig. 8c). Dieudonné further studied this case by considering first the cubic NLEVM of Craft *et al.*[37] coupled with the $k-\omega$ model. The results are even worse than with the linear model. Nonetheless, by rising the back pressure by 5% and reducing the eddy viscosity by 3/4 in the cubic NLEVM, a very good pressure distribution and lambda shape are obtained (Fig. 8d), with a slight improvement over the SST results. Second, Dieudonné tested the current WD$^+$ model with no adjustment and reproduced the better results as obtained with the ad-hoc NLEVM: the lambda shape of the shock (Fig. 8e) is comparable with the one given by the ad-hoc NLEVM (Fig. 8d),

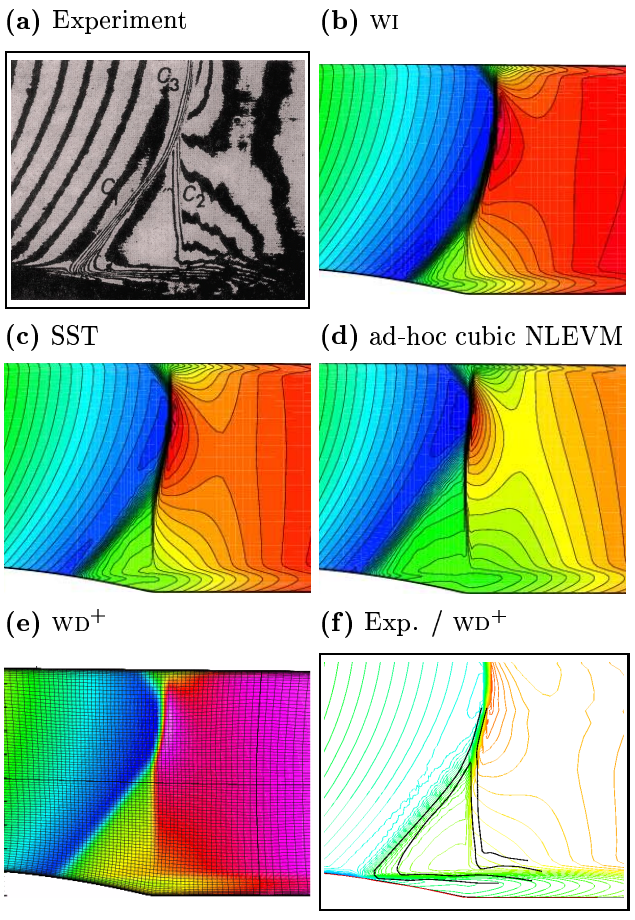

Fig. 8 Transonic bump flow in the separation region; (a): experimental interferogram, (b–e): computed isobars, (f): density isolines (wd$^+$ model) with superimposed lines from the experimental interferogram (from Ref. 34, with permission).

and a superimposition of the density field with lines extracted from the experimental interferogram (Fig. 8f) shows a very good agreement. Further details about these results, including pressure distributions and velocity profiles can be found in Ref 34.

This work supports the idea that, in the case of the transonic bump, the key-point is to lower the eddy viscosity, and consequently the TKE level in the separating flow, rather than accurately modeling the Reynolds stress anisotropy. The latter way could certainly further improve the results, but much of the work is done by the WNL correction.

Unsteady Transonic SWBLI over an Airfoil

As underlined by Dolling,[1] RANS computations with standard linear two-equation models are known to be unable to predict pressure fluctuations when the SWBLI causes the appearance of unsteadiness in the flow. An archetype of this phenomenon, which is of primary importance for aircraft wing design, is the appearance of flow oscillations induced by SWBLI over a transonic airfoil. Depending on the airfoil shape and flow conditions, Shock-Induced Oscillations (SIO) of the flow may appear, coupled with periodic extension/reduction of the separated region downstream the shock, and they can yield airfoil buffeting through the mechanical response of the wing structure.

Several experimental studies have been carried out to understand the physics of this phenomenon. McDevitt & Okuno[38] have experimentally identified the Mach-number/incidence-angle relationship for the SIO onset over the NACA0012 airfoil at Mach numbers between 0.7–0.8, incidence angles between 0–5° and chord Reynolds number between 1–14 10^6. Barakos & Drikakis[39] have shown that no combination of Mach number and incidence angle in this range can yield SIO using standard linear $k-\epsilon$ turbulence models. On the opposite, either the $k-\epsilon$ or the $k-\omega$ version of the cubic NLEVM by Craft *et al.*[37] does a good job in predicting the Mach-number/incidence-angle relationship for the SIO onset. Barakos & Drikakis have also established that by suppressing the functional dependence of c_μ on the strain and vorticity invariants in the NLEVM model, no more SIO can be obtained. They conclude that the key-point in the success of both cubic NLEVM is the functional c_μ and not the non-linear expansion of the shear stress,[39] so that it would be worthwhile to use a functional c_μ in conjunction with a linear two-equation model.

On the other hand, in the ONERA S3MA wind tunnel, unsteady pressure and skin-friction coefficients have been measured on the RA16SC1 supercritical airfoil in a flow at a Mach number of 0.732 for a chord Reynolds number of 4.2 10^6 at different angles of attack α_e.[40] SIO have been measured only for α_e between 3–5°. Inviscid/viscous coupled computations indicate that the effects of the side-wall boundary lay-

ers on the symmetry plane may be taken into account by performing the two-dimensional computations at lower Mach number (0.723) and angle of attack ($\alpha_c = \alpha_e - 1°$).[40] In the case $\alpha_e = 4°$ corresponding to the maximum amplitude in the flow oscillations (Fig. 9) and in the measured pressure fluctuations, Furlano *et al.*[41] show that no oscillation can be obtained using the Smith $k-\ell$ turbulence model[42] and that pressure oscillations appear with correct frequency and amplitudes when the $k-\ell$ linear eddy-viscosity is arbitrarily limited to an ad-hoc maximum value. A similar phenomenon is observed with a $k-\epsilon$ model[43] by Rouzeaud *et al.*[44] These results support the idea that the key-point is the limitation of the eddy-viscosity level as obtained with a linear turbulence model.

A recent numerical study contributes to assert this hypothesis. Goncalves & Houdeville[45] have assessed the effect of a WNL correction coupled either with the high-Reynolds number $k-\epsilon$ or with the $k-\omega$ turbulence models. Wall effects are modeled through a wall-law approach.[46] In the considered case of the RA16SC1 airfoil at $\alpha_e = 4°$ as described above, it has been verified that the choice of the SST correction or the WNL correction Eq. (8), both coupled with the similar transport equations (9–10), do not really matter. This is understandable because in a two-dimensional boundary layer, both invariants s and ϖ degenerate in the same limit.

Goncalves & Houdeville[45] show that with the linear turbulence models (*i.e.* without the SST correction), no unsteady fluctuations are obtained with the $k-\omega$ model, and some develop with the $k-\epsilon$ model. In the latter case however, Fig. 10a shows that the extension of the fluctuating region and the amplitude of the pressure fluctuations are clearly underestimated. The same figure shows the dramatic and beneficial effect of the SST correction with both basic turbulence models: the extension of the fluctuating region and the amplitude of the pressure fluctuations are fairly predicted by both $k-\epsilon$ and $k-\omega$ models with the WNL correction. Recent computations with a low-Reynolds number $k-\epsilon$ model[43] and a dual-time stepping method[44] confirm that the conclusion does not depend on the wall-law approach.[47]

Between $\alpha_e = 3-5°$, the SST $k-\omega$ model predicts also the measured evolution of the frequency of the oscillations while this evolution is clearly missed with the $k-\epsilon$ model (Fig. 10b). Finally, only the SST $k-\omega$ model is able to predict the observed damping of the oscillations for $\alpha_e = 5°$ (Fig. 10c).

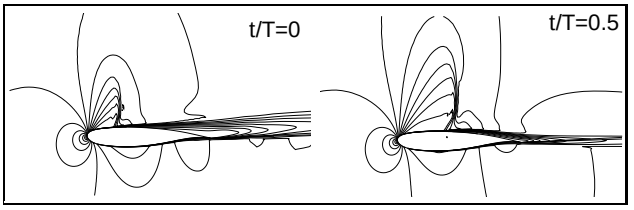

Fig. 9 RA16SC1 airfoil, SST $k-\omega$ model, Mach isolines at two instants in phase opposition (from Ref. 45, with permission).

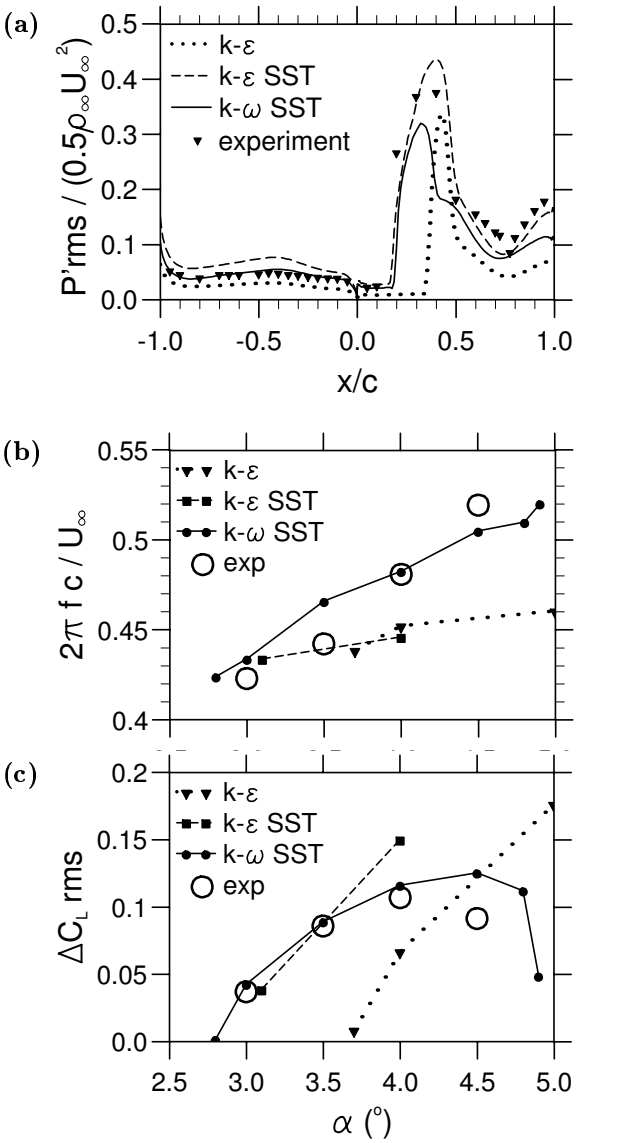

Fig. 10 RA16SC1 airfoil, (a): 4° angle of attack, root-mean-square pressure fluctuations upstream and on the suction side of the airfoil, (b): Strouhal number vs angle of attack, (c): amplitude of the lift-coefficient fluctuations vs angle of attack (from Ref. 45, with permission).

Conclusions

Usual two-equation turbulence models fail in predicting SWBLI mainly because of the linear relationship between the turbulent stress and the strain tensor through the constant value of c_μ in the definition of the eddy viscosity. Weakly Non-Linear turbulence models can be obtained very simply by considering c_μ as a functional of the strain rate and vorticity invariants. At least three different theoretical approaches all end up with a similar expression of c_μ: the generalization of the empirical Bradshaw's assumption,[19,20] the en-

forcement of the realizability principle,[21, 22] and the search for a more general effective eddy viscosity.[28]

Such a Weakly Non-Linear correction has been proposed and applied to three single sharp fin plate configurations with different SWBLI strengths. The correction yields a much better prediction of the pressure under the vortical flow formed within the lambda foot of the shock. The maximum of the skin-friction coefficient is decreased by one third, yielding levels comparable to the measurements. In the strong interaction case (Mach 4, 30.6° fin), the secondary separation due to the formation of a secondary shock appears, while it is totally absent from the solution without the correction. The turbulence intensity is more than halved in the vortical flow, which explains the decrease in skin-friction. It is experienced that when grid is refined, the levels of pressure and skin-friction coefficient do not converge at the attachment with the linear model, and do converge with the WNL correction. It is related to the grid-divergence of some terms in the linear model equations, which is cured by the correction.

Unlike the SST correction,[20] the WNL correction ensures realizability and is active in a pure irrotational strain (like when crossing a normal shock wave for instance). Nonetheless, the two-dimensional limit of the present WNL and the SST corrections are nearly the same. In a two-dimensional transonic channel flow over a bump, the WNL correction predicts the lambda-shape of the shock at least as well as the SST correction and an ad-hoc version[34] of a cubic NLEVM.[37] In transonic flows over airfoils, observed Shock-Induced Oscillations cannot be properly obtained with linear turbulence models, as shown by Barakos & Drikakis[39] with $k-\epsilon$, Furlano *et al.*[41] with $k-\ell$, Goncalves & Houdeville[45] with $k-\omega$. In all three cases, SIO can be obtained either with the cubic non-linear[37] version of the $k-\epsilon$ model,[39] an arbitrary maximum limit on the eddy viscosity[41] or the use of the WNL or SST correction.[45] Moreover, the WNL or SST $k-\omega$ model is able to predict the evolution of the frequency and amplitude of the oscillations when varying the angle of attack of the airfoil.[45] These results confirm the statement by Barakos & Drikakis:[39] in order to predict SIO over airfoils, the key-point is the functional c_μ and not the non-linear expansion of the shear stress.

The overall conclusion is that the WNL correction, originally developped for two-dimensional subsonic flows[21, 22, 24] has been successfully used in 3-D supersonic and 2-D transonic steady and unsteady flows. Some flaws still persist in the mean flow and should be further reduced by refining the c_μ functional for intermediate values of the strain and/or vorticity invariants, and by introducing either a variable turbulent Prandtl number or specific equations to further deal with the heat-transfer issue. Then, non-linear turbulence models could be considered for a better prediction of turbulent stresses.

Acknowledgements

The author is grateful to Rutgers University for welcoming him in the Department of Mechanical and Aerospace Engineering to perform the single fin computations. Especially, Prof. Doyle D. Knight is greatly acknowledged for many fruitful discussions, from which the orientation and results of the reported research come. The two-year visit in Rutgers University was supported by DGA, the French Armament Procurement Agency under grants No. DSP/SREA ERE 996053 and DSA/SPAé 9595005 BC 106. The computational resources were provided by the U.S. National Science Foundation at the National Center for Supercomputing Applications, University of Illinois at Urbana-Champaign (allocation No. CTS990067 N). Let Miss Mirna Daouk be thanked here for her help in preparing some of the computations. The analysis presented in this paper could be carried out only with the kind support of Dr. Daniel Arnal in the framework of the ONERA Federative Research Project on Supersonic Aerodynamics. The author gratefully acknowlegde Dr. Alexander A. Zheltovodov for providing the experimental results on the single fins, Dr. Walter Dieudonné and Dr. Eric Goncalves for the transonic bump and buffeting results, respectively.

References

[1]Dolling, D. S., "Fifty Years of Shock-Wave/Boundary-Layer Interaction Research: What Next?" *AIAA Journal*, Vol. 39, No. 8, 2001, pp. 1517–1531.

[2]Délery, J. M. and Panaras, A. G., "Shock-Wave/Boundary-Layer Interactions in High-Mach-Number Flows," *Hypersonic Experimental and Computational Capability, Improvement and Validation*, edited by W. S. Sarric, J. Muylaert, and C. Dujarric, AGARD AR-319, Vol. 1, May 1996, pp. 2-1–2-61.

[3]Smits, A. J. and Dussauge, J.-P., *Turbulent Shear Layers in Supersonic Flow*, AIP Press, Woodbury, New York, 1996.

[4]Knight, D. D. and Degrez, G., "Shock Wave Boundary Layer Interactions in High Mach Number Flows – A Critical Survey of Current CFD Prediction Capabilities," *Hypersonic Experimental and Computational Capability, Improvement and Validation*, edited by J. Muylaert, A. Kumar, and C. Dujarric, AGARD AR-319, Vol. 2, Dec. 1998, pp. 1-1–1-35.

[5]Knight, D. D., Horstman, C. C., Settles, G. S., and Zheltovodov, A. A., "Three-Dimensional Shock Wave/Turbulent Boundary Layer Interactions Generated by a Single Fin," *Thermophysics and AeroMechanics*, Vol. 5, No. 2, 1998, pp. 131–140.

[6]Panaras, A. G., "Algebraic Turbulence Modeling for Swept Shock-Wave/Turbulent Boundary-Layer Interactions," *AIAA Journal*, Vol. 35, No. 3, 1997, pp. 456–463.

[7]Panaras, A. G., "The Effect of the Structure of Swept Shock-Wave/Turbulent Boundary-Layer Interactions on Turbulence Modelling," *Journal of Fluid Mechanics*, Vol. 338, 1997, pp. 203–230.

[8]Zheltovodov, A. A., Maksimov, A. I., and Shevchenko, A. M., "Topology of Three-Dimensional Separation Under the Conditions of Symmetric Interaction of Crossing Shocks and Expansion Waves with Turbulent Boundary Layer," *Thermophysics and AeroMechanics*, Vol. 5, No. 3, 1998, pp. 293–312.

[9]Zheltovodov, A. A., Maksimov, A. I., Shevchenko, A. M., and Knight, D. D., "Topology of Three-Dimensional Separation Under the Conditions of Asymmetrical Interaction of Crossing Shocks and Expansion Waves with Turbulent Boundary

Layer," *Thermophysics and AeroMechanics*, Vol. 5, No. 4, 1998, pp. 483–503.

[10]Zheltovodov, A. A., Maksimov, A. I., Gaitonde, D. V., Visbal, M., and Shang, J. S., "Experimental and Numerical Study of Symmetric Interaction of Crossing Shocks and Expansion Waves with a Turbulent Boundary Layer," *Thermophysics and AeroMechanics*, Vol. 7, No. 1, 2000, pp. 155–171.

[11]Gaitonde, D. V., Shang, J. S., Garrison, T. J., Zheltovodov, A. A., and Maksimov, A. I., "Three-Dimensional Turbulent Interactions Caused by Asymmetric Crossing-Shock Configurations," *AIAA Journal*, Vol. 37, No. 12, 1999, pp. 1602–1608.

[12]Knight, D. D., Gnedin, M., Becht, R., Zheltovodov, A. A., and Maksimov, A. I., "Numerical Simulation of Crossing-Shock-Wave/Turbulent-Boundary-Layer Interaction Using a Two-Equation Model of Turbulence," *Journal of Fluid Mechanics*, Vol. 409, 2000, pp. 121–147.

[13]Thivet, F., Knight, D. D., Zheltovodov, A. A., and Maksimov, A. I., "Analysis of Observed and Computed Crossing-Shock Wave/Boundary-Layer Interactions," *Aerospace Science and Technology*, Vol. 5, No. 8, 2001.

[14]Urbin, G., Knight, D., and Zheltovodov, A. A. "Large Eddy Simulation of a Supersonic Compression Corner Part I," AIAA Paper 2000-0398, Jan. 2000.

[15]Rizzetta, D. P., R, V. M., and Gaitonde, D. V. "Direct Numerical and Large-Eddy Simulation of Supersonic Flows by a High-Order Method," AIAA Paper 2000-2408, June 2000.

[16]Rizzetta, D. and M, V. "Large Eddy Simulation of Supersonic Compression Ramp Flows," AIAA Paper 2001-2858, June 2001.

[17]Thivet, F., Knight, D. D., Zheltovodov, A. A., and Maksimov, A. I., "Insights in Turbulence Modeling for Crossing-Shock-Wave/Boundary-Layer Interactions," *AIAA Journal*, Vol. 39, No. 6, 2001, pp. 985–995.

[18]Bradshaw, P., Ferriss, D. H., and Atwell, N. P., "Calculation of Boundary-Layer Development Using the Turbulent Energy Equation," *Journal of Fluid Mechanics*, Vol. 28, No. 3, 1967, pp. 593–616.

[19]Coakley, T. J. "Turbulence Modeling Methods for the Compressible Navier-Stokes Equations," AIAA Paper 83-1693, June 1983.

[20]Menter, F. R., "Two-Equation Eddy-Viscosity Turbulence Models for Engineering Applications," *AIAA Journal*, Vol. 32, No. 8, 1994, pp. 1598–1605.

[21]Durbin, P. A., "On the $k-\epsilon$ Stagnation Point Anomaly," *International Journal of Heat & Fluid Flow*, Vol. 17, No. 1, 1996, pp. 89–90.

[22]Moore, J. G. and Moore, J. "Realizability in Two-Equation Turbulence Models," AIAA Paper 99-3779, June–July 1999.

[23]Schumann, U., "Realisability of Reynolds Stress Turbulence Models," *Physics of Fluids*, Vol. 20, No. 5, 1977, pp. 721–725.

[24]Behnia, M., Parneix, S., and Durbin, P. A., "Simulation of Jet Impingement Heat Transfer with the $k-\epsilon-v^2$ Model," *Annual Research Briefs 1996*, CTR, Stanford, California, 1996, pp. 3–16 (http://ctr.stanford.edu/ResBriefs96/behnia.ps.Z).

[25]Zheltovodov, A. A., "Regimes and Properties of Three-Dimensional Separation Flows Initiated by Skewed Compression Shocks," *Journal of Applied Mechanics and Technical Physics*, Vol. 23, No. 3, 1982, pp. 413–418.

[26]Kim, K. S., Lee, Y., Alvi, F. S., Settles, G. S., and Horstman, C. C., "Skin-Friction Measurements and Computational Comparison of Swept Shock/Boundary-Layer Interactions," *AIAA Journal*, Vol. 29, No. 10, 1991, pp. 1643–1650.

[27]Zheltovodov, A. A., Maksimov, A. I., and Schulein, E., "Development of Turbulent Separated Flows in the Vicinity of Swept Shock Waves," *The Interactions of Complex 3-D Flows*, edited by A. M. Kharitonov, Institute of Theoretical and Applied Mechanics, USSR Academy of Sciences, Siberian Division, 1987, pp. 67–91.

[28]Pope, S. B., "A More General Effective-Viscosity Hypothesis," *Journal of Fluid Mechanics*, Vol. 72, No. 2, 1975, pp. 331–340.

[29]"$\mathcal{GASP}$, General Aerodynamic Simulation Program Version 3," User's manual, AeroSoft, Inc., Blacksburg, Virginia, May 1996.

[30]Wilcox, D. C., "Reassessment of the Scale-Determining Equation for Advanced Turbulence Models," *AIAA Journal*, Vol. 26, No. 11, 1988, pp. 1299–1310.

[31]Wilcox, D. C., "Comparison of Two-Equation Turbulence Models for Boundary Layers with Pressure Gradient," *AIAA Journal*, Vol. 31, No. 8, 1993, pp. 1414–1421.

[32]Thivet, F., Daouk, M., and Knight, D. D., "Influence of the Wall Condition on $k-\omega$ Turbulence Model Predictions," *AIAA Journal*, Vol. 40, No. 1, pp. 179–181.

[33]Délery, J. M., "Experimental Investigation of Turbulent Properties in Transonic Shock/Boundary-Layer Interactions," *AIAA Journal*, Vol. 21, No. 2, 1983, pp. 180–185.

[34]Dieudonné, W., *Anisotropic Turbulence Modeling in Compressible Flows and Applications to Aerospike Plug Nozzles*, Ph.D. thesis, VKI, Nov. 2000.

[35]Délery, J. M., "Contribution of Laser Doppler Velocimetry to the Physical Description of Shock-Wave/Turbulent Boundary-Layer Interactions with Incidence on Turbulence Modelling," *Shock-Wave/Boundary-Layer Interactions in Supersonic and Hypersonic Flows*, AGARD R-792, Aug. 1993, pp. 5-1–5-34.

[36]Batten, P., Loyau, H., and Leschziner, M. A., editors, "ERCOFTAC Workshop on Shock/Boundary-Layer Interaction," Mar. 1997.

[37]Craft, T. J., Launder, B. E., and Suga, K., "Development and Application of a Cubic Eddy-Viscosity Model of Turbulence," *International Journal of Heat & Fluid Flow*, Vol. 17, No. 2, 1996, pp. 108–115.

[38]McDevitt, J. B. and Okuno, A. F., "Static and Dynamic Pressure Measurements on a NACA 0012 Airfoil in the Ames High Reynolds Number Facility," NASA TP-2485, June 1985.

[39]Barakos, G. and Drikakis, D., "Numerical Simulation of Transonic Buffet Flows Using Various Turbulence Closures," *International Journal of Heat & Fluid Flow*, Vol. 21, No. 5, 2000, pp. 620–626.

[40]Benoit, B. and Legrain, I. "Buffeting Prediction for Transport Aircraft Applications Based on Unsteady Pressure Measurements," AIAA Paper 87-2350, Aug. 1987.

[41]Furlano, F., Coustols, E., Plot, S., and Rouzeaud, O., "Steady and Unsteady Computations of Flows Close to Airfoil Buffeting: Validation of Turbulence Models," Second International Symposium on Turbulent and Shear Flow Phenomena, June 2001.

[42]Smith, F. T., "Theoretical Aspects of Transition and Turbulence in Boundary Layers," *AIAA Journal*, Vol. 31, No. 12, Dec. 1993, pp. 2220–2226.

[43]Jones, W. P. and Launder, B. E., "The Calculation of Low-Reynolds-Number Phenomena with a Two-Equation Model of Turbulence," *International Journal of Heat and Mass Transfer*, Vol. 16, 1973, pp. 1119–1130.

[44]Rouzeaud, O., Plot, S., and Couaillier, V., "Numerical Simulations of Buffeting over Airfoil Using Dual-Time Stepping Method," European Congress on Computational Methods in Applied Sciences and Engineering ECCOMAS, Sept. 2000.

[45]Goncalves, E. and Houdeville, R. "Numerical Simulation of Shock Oscillations Over an Airfoil Using a Wall Law Approach," AIAA Paper 2001-2857, June 2001.

[46]Goncalves, E. and Houdeville, R., "Reassessment of the Wall Functions Approach for RANS Computations," *Aerospace Science and Technology*, Vol. 5, No. 1, 2001, pp. 1–14.

[47]Goncalves, E., Furlano, F., Houdeville, R., and Coustols, E., "Unsteady RANS Computations: Simulation of the Buffeting over an Airfoil," IUTAM Symposium on Unsteady Separated Flows, Apr. 2002.